Interactions of zearalenone and its reduced metabolites α-zearalenol and β-zearalenol with serum albumins: species differences, binding sites, and thermodynamics

Zelma Faisal,[1,2] Beáta Lemli,[2,3,4] Dénes Szerencsés,[3] Sándor Kunsági-Máté,[2,3,4] Mónika Bálint,[5] Csaba Hetényi,[5] Mónika Kuzma,[6] Mátyás Mayer,[6] Miklós Poór [1,2,*]

[1]Department of Pharmacology, University of Pécs, Faculty of Pharmacy, Szigeti út 12, Pécs H-7624, Hungary

[2]János Szentágothai Research Center, Ifjúság útja 20, Pécs H-7624, Hungary

[3]Department of General and Physical Chemistry, University of Pécs, Faculty of Sciences, Ifjúság útja 6, Pécs H-7624, Hungary

[4]Department of Pharmaceutical Chemistry, University of Pécs, Faculty of Pharmacy, Rókus u. 2, Pécs H-7624, Hungary

[5]Department of Pharmacology and Pharmacotherapy, University of Pécs, Medical School, Szigeti út 12, Pécs H-7624, Hungary

[6]Department of Forensic Medicine, Medical School, University of Pécs, Szigeti út 12, Pécs H-7624, Hungary

*Corresponding author: Miklós Poór, PharmD, PhD

Department of Pharmacology, University of Pécs, Faculty of Pharmacy, Szigeti út 12, H-7624 Pécs, Hungary

Phone: +36-72-536-000/31646

Fax: +36-72-536-218

E-mail address: poor.miklos@pte.hu

Abstract

Zearalenone (ZEN) is a mycotoxin produced by *Fusarium* species. ZEN mainly appears in cereals and related foodstuffs, causing reproductive disorders in animals, due to its xenoestrogenic effects. The main reduced metabolites of ZEN are α-zearalenol (α-ZEL) and β-zearalenol (β-ZEL). Similarly to ZEN, ZELs can also activate estrogen receptors, moreover, α-ZEL is the most potent endocrine disruptor among these three compounds. Serum albumin is the most abundant plasma protein in the circulation, it affects the tissue distribution and elimination of several drugs and xenobiotics. Although ZEN binds to albumin with high affinity, albumin-binding of α-ZEL and β-ZEL has not been investigated. In this study, the complex formation of ZEN, α-ZEL, and β-ZEL with human (HSA), bovine (BSA), porcine (PSA), and rat serum albumins (RSA) was investigated by fluorescence spectroscopy, affinity chromatography, thermodynamic studies, and molecular modeling. Our main observations are as follows: (1) ZEN binds with higher affinity to albumins than α-ZEL and β-ZEL. (2) The low binding affinity of β-ZEL towards albumin may result from its different binding position or binding site. (3) The binding constants of the mycotoxin-albumin complexes significantly vary with the species. (4) From the thermodynamic point of view, the formation of ZEN-HSA and ZEN-RSA complexes are similar, while the formation of ZEN-BSA and ZEN-PSA complexes are markedly different. These results suggest that the toxicological relevance of ZEN-albumin and ZEL-albumin interactions may also be species-dependent.

Keywords: zearalenone; zearalenols; serum albumin; species-dependent alternations; fluorescence spectroscopy

Introduction

Zearalenone (ZEN; Fig. 1) is a *Fusarium*-derived mycotoxin, which occurs as a contaminant in cereals (e.g., maize, wheat, or barley), spices, milk, and beer (Yazar and Omurtag 2008; Maragos 2010). Because ZEN is a xenoestrogen, it induces reproductive disorders in farm animals (EFSA, 2017; Shier et al. 2001). After its absorption from the gastrointestinal tract, ZEN is extensively biotransformed, during which reduced metabolites and glucuronic acid conjugates are formed (EFSA, 2017). Most important reduced derivatives of ZEN are α-zearalenol (α-ZEL) and β-zearalenol (β-ZEL) (Fig. 1), however, lower amounts of zearalanone, α-zearalanol, and β-zearalanol are produced as well (Minervini and Dell'Aquila 2008). ZELs also bind with high affinity to estrogen receptors, α-ZEL even exerts significantly stronger toxic effect than the parent compound ZEN (Fleck et al. 2017; Frizzell et al. 2011; Filannino et al. 2011). Besides ZEN, the appearance of ZELs has been also reported in some foodstuffs, including milk and soy meal (Huang et al. 2014; Schollenberger et al. 2006). ZEN and its metabolites are rapidly absorbed from the gastrointestinal tract and distributed among several organs/tissues; glucuronic acid conjugates of ZEN and ZELs are excreted through the biliary route then undergo enterohepatic circulation (EFSA, 2017).

Serum albumin is the most abundant plasma protein in the circulation. Albumin maintains the oncotic pressure of blood as well as it has important buffer, antioxidant, and pseudo-enzymatic functions. Albumin forms non-covalent complexes with several endogenous compounds, drugs, and xenobiotics, affecting significantly their tissue distribution and plasma elimination half-life (Fanali et al. 2012; Yamasaki et al. 2013). Albumin is built up from three domains (I, II, and III), each domain contains two subdomains (A and B). The two major binding sites of albumin are located in subdomain IIA (Sudlow's Site I) and subdomain IIIA (Sudlow's Site II). However, recent studies highlighted the importance of a third binding site located in subdomain IB (Heme binding site) (Fanali et al. 2012; Zsila 2013). As previous

studies demonstrated, many mycotoxins (e.g., aflatoxins, citrinin, deoxynivalenol, ochratoxins, patulin, and ZEN) form stable non-covalent complexes with albumins (Poór et al. 2012, 2015, 2017a, 2017b; Li et al. 2013; Perry et al. 2003; Yuqin et al. 2014). Some of these interaction could be of high toxicological importance. Aflatoxins, deoxynivalenol, and patulin form less stable complexes with human albumin ($K \sim 10^4$ L/mol) (Poór et al. 2017a; Li et al. 2013; Yuqin et al. 2014) than citrinin and ZEN ($K \sim 10^5$ L/mol) (Poór et al. 2015, 2017b), while the stability of ochratoxin A-albumin complex is extremely high ($K \sim 10^7$ L/mol) (Kőszegi and Poór 2016; Sueck et al., 2018).

As demonstrated in our previous study, ZEN binds to human albumin with high affinity, occupying a non-conventional binding site between subdomains IIA and IIIA (Poór et al. 2017b). In another study, Ma et al. investigated the complex formation of ZEN with bovine albumin (Ma et al. 2018). Based on these two studies, the complex formation of ZEN with human and bovine albumins shows large differences. Therefore, the investigation of species-dependence of ZEN-albumin interactions seems reasonable. Furthermore, while ZEN is known to bind to albumin with high affinity, we have no information regarding the interactions of α- and β-ZEL with serum albumin.

In this study, the interactions of ZEN, α-ZEL, and β-ZEL with human (HSA), bovine (BSA), porcine (PSA), and rat (RSA) serum albumins were investigated using fluorescence spectroscopy in order to determine the binding constants of mycotoxin-albumin complexes by fluorescence quenching method. The mycotoxin-HSA interactions were also evaluated by high performance affinity chromatography (HPAC). To characterize further the species-dependence of the albumin-binding of ZEN, thermodynamic studies were performed. Finally, mycotoxin-albumin interactions were also examined employing molecular modeling studies. Our results demonstrate that α-ZEL and especially β-ZEL binds with significantly lower

affinity to albumin than ZEN, and albumin-binding of each mycotoxin (ZEN, α-ZEL, and β-ZEL) show very significant species-dependence.

Materials and methods

Reagents

All reagents and solvents were spectroscopic or analytical grade. Zearalenone (ZEN; MW = 318.36 g/mol), α-zearalenol (α-ZEL; MW = 320.38 g/mol), β-zearalenol (β-ZEL; MW = 320.38 g/mol), human serum albumin (HSA; MW = 66.4 kDa), bovine serum albumin (BSA; MW = 66.4 kDa), porcine serum albumin (PSA; MW = 67.5 kDa), rat serum albumin (RSA; MW = 64.6 kDa), and warfarin were purchased from Sigma-Aldrich. Stock solutions of mycotoxins (5000 μmol/L; ZEN: 1.592 g/L; ZELs: 1.601 g/L) were prepared in ethanol (VWR, spectroscopic grade) and stored at –20°C.

Spectroscopic measurements

Fluorescence and absorption spectra were recorded employing a Hitachi F-4500 fluorimeter (Tokyo, Japan) and a Specord Plus 210 (Analytic Jena AG, Jena, Germany) UV-Vis spectrophotometer, respectively. Mycotoxin-albumin interactions were investigated in phosphate buffered saline (PBS: 8.00 g/L NaCl, 0.20 g/L KCl, 1.81 g/L Na_2HPO_4 x $2H_2O$, 0.24 g/L KH_2PO_4; pH = 7.4). Spectroscopic measurements were carried out in the presence of air, at +25°C (except thermodynamic studies).

Complex formation of ZEN and its reduced metabolites with serum albumins was examined based on fluorescence quenching effects of the mycotoxins, applying the Stern-Volmer equation:

$$\frac{I_0}{I} = 1 + K_{SV} \times [Q] \qquad (1)$$

where I and I_0 are the emission intensities of albumins with and without mycotoxins, respectively. K_{SV} (unit: L/mol) is the Stern-Volmer quenching constant and $[Q]$ is the molar concentration of the quencher (ZEN or ZELs). To eliminate the inner-filter effects of mycotoxins, emission intensities were corrected based on the following equation (Poór et al. 2017a):

$$I_{cor} = I_{obs} \times e^{(A_{ex}+A_{em})/2} \quad (2)$$

where I_{cor} and I_{obs} denote the corrected and observed emission intensities, respectively; while A_{ex} and A_{em} are the absorbance of mycotoxins at 295 and 340 nm, respectively.

Binding constants (K; unit: L/mol) of mycotoxin (MT)-serum albumin (SA) complexes were calculated by non-linear fitting using Hyperquad2006 program package (Poór et al. 2018; Sueck et al., 2018), during which the following equations were implemented in the Hyperquad code:

$$pSA + qMT \leftrightarrow SA_pMT_q \quad (3)$$

$$\beta_{pq} = \frac{[SA_pMT_q]}{[SA]^p[MT]^q} \quad (4)$$

where p and q denote the coefficients which indicate the stoichiometry associated with the equilibrium. All equilibrium constants (β) were defined as overall binding constants.

$$SA + MT \leftrightarrow SA\,MT \quad \beta_1 = \frac{[SA\,MT]}{[SA][MT]} \quad (5)$$

$$SA + qMT \leftrightarrow SA\,MT_q \quad \beta_q = \frac{[SA\,MT_q]}{[SA][MT]^q} \quad (6)$$

The relationship between the overall binding constants and the stepwise binding constants was calculated by Hyperquad based on the followings.

$$\beta_1 = K_1;\ \beta_q = K_1 \times K_2 \ldots \times K_q \quad (7)$$

The stoichiometry and binding constants of mycotoxin-albumin complexes were determined by the model associated with the lowest standard deviation.

High performance affinity chromatography (HPAC)

Mycotoxin-HSA complex formation was confirmed by HPAC analyses at room temperature. The HPLC system (Jasco) was equipped with an intelligent pump (PU-980), a degasser (DG-2080-54), a manual injector with a 5 µl-sample loop and a diode-array detector (MD 2010 Plus). Data were recorded and evaluated by ChromNAV Software. The eluent which contained isopropanol (HPLC grade, VWR) and 0.01 mol/L pH 7.0 ammonium acetate buffer (15:85 v/v%) was pumped with 0.5 mL/min flow rate through an injector (Rheodyne 7725i) and the HPAC column coated with immobilized HSA (50 x 3.0 mm, 5 µm particle size, Chiralpak® HSA). The isocratically eluted compounds were detected by diode-array detector at 235 nm.

Thermodynamic studies

In the thermodynamic studies, fluorescence spectra were recorded using Fluorolog τ3 spectrofluorometric system (Jobin-Yvon/SPEX) at six different temperatures (298, 301, 304, 307, 310, and 313 K). Based on our earlier work (Poór et al. 2017b), binding constants of ZEN-albumin complexes were calculated applying Hyperquad2006 program package (Gans et al. 1996) assuming 1:1 stoichiometry. Thermodynamic parameters associated to the complex formations between ZEN and albumins were computed using the van't Hoff equation:

$$logK = -\frac{\Delta G}{RT} = -\frac{\Delta H}{2.303 \cdot R \cdot T} + \frac{\Delta S}{2.303 \cdot R} \qquad (8)$$

where *ΔG*, *ΔH*, and *ΔS* reflect the Gibbs free energy, enthalpy, and entropy changes of the binding reaction, respectively; while *R* is the gas constant and *T* refers the temperature.

Modeling studies

The ligand molecules (α-ZEL and β-ZEL) were built in Maestro (Schrödinger 2013). The raw structure was energy minimized, using the semi-empirical quantum chemistry program

package, MOPAC (Stewart 1990) and the PM6 parameterization. The gradient norm was set to 0.001. The energy minimized structure was subjected to force calculations. The force constant matrices were positive definite. Apo crystallographic structure (PDB code: 1ao6) was used as a target molecule in our calculations. Acetyl and amide capping groups were attached to the N- and C-termini, respectively, using the Schrödinger Maestro program package v. 9.6 (Schrödinger 2013). As 1ao6 contains a homodimer structure, only chain A was used for calculations. Co-crystallized ions and water molecules were removed before minimizing the protein structure. The target molecule was minimized using a two-step protocol with the GROMACS software package (Abraham et al. 2015), including a steepest descent and a conjugate gradient step, using AMBER99-ildn force field (Lindorff-Larsen et al. 2010). Exit tolerance levels were set to 1000 and 10 kJ mol^{-1} nm^{-1} while maximum step sizes were set to 0.5 and 0.05 nm, respectively.

Using the optimized ligand and target structures, blind docking calculations were performed with AutoDock 4.2 program package (Morris et al. 2009) as described in our previous publications (Hetényi and van der Spoel 2002, 2006, 2011). Gasteiger-Marsilli partial charges were added to both ligands and target atoms using AutoDock Tools (Morris et al. 2009) and a united atom representation was applied for non-polar moieties. A grid box of 250 grid points was assigned in all axes, and 0.375 Å spacing was calculated and centered on the center of mass of the target by AutoGrid 4.2. Lamarckian genetic algorithm was used for global search. Flexibility at three active torsions was allowed on both ligands. Number of docking runs was set to 100, numbers of energy evaluations and generations were 20 million (Hetényi and van der Spoel 2002). The docked ligand copies were ordered according to AutoDock 4 scores (Morris et al. 2009), and subsequently clustered using a 2 Å distance tolerance between cluster representatives.

Results and discussion

Investigation of mycotoxin-albumin interactions using fluorescence quenching method

In this study, fluorescence emission spectra of albumins (2 μmol/L; HSA/BSA: 0.133 g/L; PSA/RSA: 0.135 g/L) were recorded in the presence of increasing mycotoxin concentrations (0-10 μmol/L; ZEN: 0.000-3.184 mg/L; ZELs: 0.000-3.204 mg/L) in PBS buffer (pH = 7.4; λ_{ex} = 295 nm). In order to exclude the inner-filter effect, emission intensities were corrected by Eq. 2. In a concentration-dependent fashion, each tested mycotoxin induced the decrease of fluorescence at 340 nm (emission maximum of albumins), resulted from the quenching effects of ZEN and ZELs on albumins and suggesting the formation of mycotoxin-albumin complexes (Poór et al. 2015, 2017a, 2017b). The Stern-Volmer plots of mycotoxin-albumin complexes showed good linearity (Fig. 2; R^2 = 0.97-0.99). Based on the mycotoxin-induced quenching of fluorescence, Stern-Volmer quenching constants (K_{SV}) and binding constants (K) of mycotoxin-albumin complexes were calculated (see details in *Spectroscopic measurements* section). Both Stern-Volmer equation (Eq. 1) and Hyperquad2006 program (Eqs. 3-7) suggest 1:1 stoichiometry of complex formation. As demonstrated in Table 1, logK_{SV} and log$K$ values correlate, and suggest the formation of stable mycotoxin-albumin complexes (log$K$ = 4.05-5.43). Judged from the logK_{SV} and log$K$ values, HSA, BSA, and PSA form the most stable complexes with ZEN followed by α-ZEL and β-ZEL, while each mycotoxin bind to RSA with similar affinity. The binding constant of ZEN-HSA complex is 2.3-fold and 5.8-fold higher compared to α-ZEL-HSA and β-ZEL-HSA, respectively. ZEN and ZELs formed by far the most stable complexes with RSA, while the least stable mycotoxin-albumin complexes were typically formed with PSA. Significant species differences were observed in binding to albumin with each mycotoxin tested, approaching 10-fold or higher differences when comparing the stabilities of ZEN-PSA vs. ZEN-RSA, α-ZEL-BSA vs. α-ZEL-RSA, or β-ZEL-HSA vs. β-ZEL-RSA, for example. These results suggest that

220 the influence of albumin on the toxicokinetics of ZEN and ZELs may also be species-
221 dependent.
222
223 *High performance affinity chromatography of ZEN and ZELs*
224 HPAC column coated with immobilized HSA was applied to confirm the results of our
225 fluorescence spectroscopic studies. Because the data in Table 1 indicate that ZEN and ZELs
226 bind with significantly different affinities to HSA, it is reasonable to expect that these
227 compounds are eluted from the HSA-HPAC column at different retention times. Applying the
228 suggested experimental conditions of the column, we tried to elute the mycotoxins both with
229 0.01 mol/L ammonium acetate (pH 7.0) and with 0.01 mol/L sodium phosphate (pH 7.0)
230 buffers containing isopropanol (5-15 v/v%). In the sodium phosphate buffer, elution of ZEN
231 was excessively delayed, therefore, further experiments were performed with the ammonium
232 acetate buffer containing 15 v/v% isopropanol. The significant differences in the retention
233 times of ZEN, α-ZEL, and β-ZEL (Fig. 3) clearly indicate the different binding affinities of
234 these mycotoxins towards HSA. At pH 7.0, the longest retention time was observed for ZEN
235 (15.6 min), while α-ZEL (8.1 min) and β-ZEL (4.6 min) were eluted more rapidly from the
236 HSA-coated column. These results are in agreement with the spectroscopic studies, which
237 yielded the following complex stabilities: ZEN-HSA > α-ZEL-HSA > β-ZEL-HSA (Table 1).
238
239 *Thermodynamic studies*
240 Serum albumins are multifunctional proteins which are highly conserved in both sequence
241 and structure (Chruszcz et al. 2013). Therefore, it is expected that their biological behaviors,
242 such as their ligand binding properties, are usually very similar. Indeed, the mycotoxin
243 aflatoxin B1 and citrinin bind to different albumins with similar affinity (Poór et al. 2015,
244 2017a). Nevertheless, some ligands, such as ochratoxin A, show marked species-dependence

(Poór et al. 2014; Kőszegi and Poór 2016). Therefore, the interactions of ZEN with different serum albumins have been analyzed in details. Since the binding constants of ZEN to albumin from various species differ substantially (Table 1), the temperature-dependence of the ZEN-albumin complex formation, using HSA, BSA, PSA, and RSA was also examined. Fig. 4 demonstrates the van't Hoff plot of ZEN-albumin complexes, based on equilibrium constants determined at different temperatures. Thermodynamic parameters were calculated from the slope and the intercept after linear fitting (according to Eq. 8). The negative ΔG values suggest spontaneous interaction of ZEN with albumins at room-temperature (Table 2). These values are in the typical range of non-covalent interactions. During the formation of protein-ligand complexes, the interaction forces are derived from van der Waals interactions, hydrophobic forces, multiple hydrogen bonds, and/or electrostatic interactions. Thermodynamic data give deeper insights into the nature of these binding forces (Ross and Subramanian 1981). Comparing enthalpy and entropy values raised during the formation of ZEN-albumin complexes, the higher enthalpy change is associated with smaller entropy gain resulting in an enthalpy driven process regarding ZEN-HSA and ZEN-RSA complexes in agreement with the known enthalpy-entropy compensation. Negative values of both enthalpy and entropy changes indicate that van der Waals forces and hydrogen bond formation are involved in the complex formation of ZEN with HSA and RSA. Furthermore, the low entropy gain of these interactions reflects that ZEN may keep its solvation shell during the complex formation processes.

The formation of ZEN-BSA and ZEN-PSA complexes is entropy driven, in which smaller enthalpy changes are associated with higher entropy gain, showing enthalpy-entropy compensation. The positive values of entropy changes suggest the partial decomposition of the solvation shell of the interacting molecules and/or local changes (e.g., unfolding) in the conformation of albumin. The negative enthalpy change is associated with positive entropy

change, suggesting the role of electrostatic forces in the formation of ZEN-BSA and ZEN-PSA complexes. According to these thermodynamic data, the binding characteristics of the more stable ZEN-RSA and ZEN-HSA complexes seem different from those of the less stable ZEN-BSA and ZEN-PSA.

HSA and BSA are extensively studied macromolecules. Due to their structural similarity, the significantly cheaper BSA is more commonly applied to examine albumin-ligand interactions than HSA (Poór et al. 2014). However, some previous studies demonstrated that major differences may occur between HSA and BSA complexes; e.g. ochratoxin A binds to HSA with approximately 10 times higher affinity than to BSA (Poór et al. 2014). The present study gives a new example, when ligand binding shows significant species differences, as related by both the dissimilar binding constants and binding characteristics of ZEN-HSA and ZEN-BSA complexes.

To further analyze the differences between HSA and BSA, the effect of ionic strength on the ZEN-HSA and ZEN-BSA interactions were also investigated in different sodium phosphate buffers (0.05-0.53 mol/L), as it is well-known that variations in ionic strength affect the albumin-ligand interactions (Kaspchak et al. 2018). High ionic strength may decrease or increase the binding constant, depending on the involvement of electrostatic or hydrophobic forces, respectively. Fig. 5 demonstrates binding constants of ZEN-HSA and ZEN-BSA complexes as a function of the ionic strength. Although the ionic strength of the media slightly affects the binding constant of the ZEN-HSA and ZEN-BSA complexes, the different binding characteristics of the two albumin species with ZEN is apparent. At an increased ionic strength higher binding affinity was observed, reflecting dominance of hydrophobic interaction between ZEN and HSA. This means that the positive entropy change associated with hydrophobic processes is also balanced by the negative contribution of entropy change caused by formation of hydrogen bonds and action of van der Waals forces (Ross and

Subramanian 1981). Therefore, hydrophobic interactions play an important role in the complex formation of ZEN with HSA. However, the investigation of ZEN-BSA interaction did not reveal a clear correlation between the ionic strength and the binding constant (Fig. 5). In the study of Ma et al. (Ma et al. 2018) on ZEN-BSA interaction, similar observations were made. Based on positive the entropy change, they proposed that hydrophobic forces played a major role, although it is held that positive entropy change with a negative enthalpy change is suggestive for the involvement of electrostatic interactions (Ross and Subramanian 1981). Considering that the partial decomposition of solvation shells of the interacting molecules facilitates hydrophobic interactions, our observation that the binding constant of ZEN-BSA complex is independent of the ionic strength suggests the involvement of hydrophobic and electrostatic interactions.

Molecular modeling studies

First, the similarities between HSA and three other albumins from other species (BSA, PSA, and RSA) were analyzed. Initially, Uniprot alignment of bovine (BSA), porcine (PSA), and rat (RSA) serum albumins were performed compared to HSA. The results of alignment (Fig. S1) and overall statistics (Table 3) demonstrate high similarities between serum albumins from the four species. The binding site of ZEN on HSA was described in our previous publication (Poór et al. 2017b). In the present study, the amino acid composition in the corresponding binding region was compared for HSA, BSA, PSA, and RSA (Fig. S1). The ZEN binding site in HSA, BSA, and PSA contains identical amino acids (Fig. S1), while RSA contains different amino acids at positions 205 and 478: charged K (lysine) is replaced by a bulkier, but also positively charged R (arginine), while T (threonine) is replaced by S (serine), maintaining the hydroxyl group within the binding site. These minor structural differences in

RSA might be responsible for the observation that ZEN and ZELs bind much higher affinity to RSA compared to other albumins tested.

Thereafter, the available X-ray structures of BSA (4f5s) and HSA (1ao6) were compared. After their CA alignment of these two structures (Fig. S2, left), a 1.2 Å RMSD was obtained, which also demonstrates high similarity of the structures. Identical amino acids and similar amino acid conformations were observed in the binding site of ZEN in HSA and BSA (Fig. S2, right).

Using the docking parameters described in our previous publication (Poór et al. 2017b), blind docking of α-ZEL and β-ZEL was performed on HSA. Then these results were compared with previous docking studies performed with ZEN (Fig. 6A). As Fig. 6 demonstrates, the binding site and binding position of α-ZEL (obtained in the first rank) on HSA were very similar those of ZEN. However, this binding site was obtained only in the seventh rank for β-ZEL (Fig. 6C). The binding site of β-ZEL with the highest binding energy (ranking the first after blind docking) was found at approximately 15 Å away from the binding site of ZEN (Fig. 7). The similar binding site and position of α-ZEL on HSA explain why the affinity of α-ZEL toward HSA is relatively close to ZEN. However, the much weaker interaction of β-ZEL with HSA (compared to ZEN and α-ZEL) may result from a different binding position of β-ZEL in the same binding site (Fig. 6C) or from a different binding site of β-ZEL, which is also located between subdomains IIA and IIIA (Fig. 7). Nevertheless, modeling studies demonstrated that, similarly to ZEN, α- and β-ZEL also occupy non-conventional binding site(s) on HSA.

Effects of ZEN and its reduced metabolites on warfarin-HSA interaction

Our previous study demonstrated that ZEN interacts allosterically with Sudlow's Site I ligands, thus increasing the binding affinity of warfarin towards HSA (Poór et al. 2017b). Since the albumin-bound warfarin expresses much stronger fluorescence than free warfarin,

the increase in the HSA-bound warfarin significantly enhance its fluorescence at 379 nm (Poór et al. 2015, 2017a, 2017b). To test whether or not ZELs exert similar effects, ZELs at increasing concentrations (0-10 μmol/L) were added to warfarin (1 μmol/L; 0.308 mg/L) and HSA (3.5 μmol/L; 0.233 g/L) in PBS. As Fig. 8 demonstrates, α-ZEL induced a smaller rise in the fluorescence signal of warfarin-HSA complex than ZEN. In contrast, β-ZEL caused concentration-dependent decrease in the fluorescence intensity of warfarin. Under the applied conditions, free or HSA-bound ZEN and ZELs gave negligible fluorescence as compared to warfarin-HSA complex, and the very slight inner-filter effect of mycotoxins was corrected based on Eq. 2. Therefore, the observed changes in fluorescence likely resulted from the changes in the bound fraction of warfarin in the presence of these mycotoxins. The different effect of β-ZEL further support the hypothesis that binding site or position of β-ZEL is different than that of ZEN and α-ZEL.

In conclusion, fluorescence spectroscopic and HPAC studies on the interactions of ZEN, α-ZEL, and β-ZEL with HSA indicated that mycotoxin-albumin complexes were formed and their stabilities decreased in the order: ZEN-HSA > α-ZEL-HSA > β-ZEL-HSA. The lower binding affinity of β-ZEL (compared to ZEN and α-ZEL) may have resulted from its different binding position or binding site on HSA. Furthermore, when comparing albumins from various species (i.e., HSA, BSA, PSA, and RSA), significant differences of ZEN-albumin and ZEL-albumin interactions were observed, even exceeding 10-fold differences in the binding constants. ZEN and ZELs typically formed the most stable complexes with RSA and the less stable complexes with PSA. Thermodynamic studies also revealed significant species differences in ZEN-albumin interactions: the binding characteristics of ZEN to HSA and RSA were similar, whereas the binding forces involved in ZEN-BSA and ZEN-PSA complex formation appear different. Thus, the *in vivo* toxicological relevance of ZEN-albumin and ZEL-albumin interactions may also be different in various species.

Source of Funding

This project was supported by the Hungarian National Research, Development and Innovation Office (FK125166) (M.P.). The work of M.B. and C.H. is supported by the Hungarian National Research, Development and Innovation Office (K123836).

Acknowledgements

This project was supported by the János Bolyai Research Scholarship of the Hungarian Academy of Sciences (M.P.). M.P. is thankful for support of the University of Pécs for grant in the frame of Pharmaceutical Talent Centre program. This work was supported by the by the GINOP-2.3.2-15-2016-00049 grant. We acknowledge a grant of computer time from CSCS Swiss National Supercomputing Centre, and NIIF Hungarian National Information Infrastructure Development Institute. We acknowledge that the results of this research have been achieved using the DECI resource Archer based in the UK at the National Supercomputing Service with support from the PRACE aisbl. M.B. and C.H. are thankful to the University of Pécs for the grant in the frame of "Supporting Individual Research and Innovation Activity of Young Researchers, 2018" program.

Conflicts of interest: The authors declare no conflict of interest. We have full control of all primary data and we agree to allow the journal to review our data if requested.

References

Abraham MJ, Murtola T, Schulz R, Páll S, Smith JC, Hess B, Lindahl E (2015) GROMACS: high performance molecular simulations through multi-level parallelism from laptops to supercomputers. SoftwareX 1:19-25. https://doi.org/10.1016/j.softx.2015.06.001

Chruszcz M, Mikolajczak K, Mank N, Majorek KA, Porebski PJ, Minor W (2013) Serum albumins - unusual allergens. Biochim Biophys Acta 1830:5375-5381. https://doi.org/10.1016/j.bbagen.2013.06.016

European Food Safety Authority (EFSA) (2017) Risks for animal health related to the presence of zearalenone and its modified forms in feed. EFSA Journal 15:4851. https://doi.org/10.2903/j.efsa.2017.4851

Fanali G, Di Masi A, Trezza V, Marino M, Fasano M, Ascenzi P (2012) Human serum albumin: From bench to bedside. Mol Aspects Med 33:209-290. https://doi.org/10.1016/j.mam.2011.12.002

Filannino A, Stout TA, Gadella BM, Sostaric E, Pizzi F, Colenbrander B, Dell'Aquila ME, Minervini F (2011) Dose-response effects of estrogenic mycotoxins (zearalenone, alpha- and beta-zearalenol) on motility, hyperactivation and the acrosome reaction of stallion sperm. Reprod Biol Endocrinol 9:134. https://doi.org/10.1186/1477-7827-9-134

Fleck SC, Churchwell MI, Doerge DR (2017) Metabolism and pharmacokinetics of zearalenone following oral and intravenous administration in juvenile female pigs. Food Chem Toxicol 106:193-201.
https://doi.org/10.1016/j.fct.2017.05.048

Frizzell C, Ndossi D, Verhaegen S, Dahl E, Eriksen G, Sørlie M, Ropstad E, Muller M, Elliott CT, Connolly L (2011) Endocrine disrupting effects of zearalenone, alpha- and beta-zearalenol at the level of nuclear receptor binding and steroidogenesis. Toxicol Lett 206:210-217.
https://doi.org/10.1016/j.toxlet.2011.07.015

Gans P, Sabatini A, Vacca A (1996) Investigation of equilibria in solution. Determination of equilibrium constants with the HYPERQUAD suite of programs. Talanta 43:1739-1753.
https://doi.org/10.1016/0039-9140(96)01958-3

Hetényi C, van der Spoel D (2002) Efficient docking of peptides to proteins without prior knowledge of the binding site. Protein Sci 11:1729-1737.
https://doi.org/10.1110/ps.0202302

Hetényi C, van der Spoel D (2006) Blind docking of drug-sized compounds to proteins with up to a thousand residues. FEBS Lett 580:1447-1450.
https://doi.org/10.1016/j.febslet.2006.01.074

Hetényi C, van der Spoel D (2011) Toward prediction of functional protein pockets using blind docking and pocket search algorithms. Protein Sci 20:880-893.
https://doi.org/10.1002/pro.618

Huang LC, Zheng N, Zheng BQ, Wen F, Cheng JB, Han RW, Xu XM, Li SL, Wang JQ (2014) Simultaneous determination of aflatoxin M1, ochratoxin A, zearalenone and α-zearalenol in milk by UHPLC-MS/MS. Food Chem 146:242-249. https://doi.org/10.1016/j.foodchem.2013.09.047

Kaspchak E, Mafra LI, Mafra MR (2018) Effect of heating and ionic strength on the interaction of bovine serum albumin and the antinutrients tannic and phytic acids, and its influence on in vitro protein digestibility. Food Chem 252:1-8. https://doi.org/10.1016/j.foodchem.2018.01.089

Kőszegi T, Poór M (2016) Ochratoxin A: Molecular interactions, mechanisms of toxicity and prevention at the molecular level. Toxins 8:111. https://doi.org/10.3390/toxins8040111

Li Y, Wang H, Jia B, Liu C, Liu K, Qi Y, Hu Z (2013) Study of the interaction of deoxynivalenol with human serum albumin by spectroscopic technique and molecular modelling. Food Addit Contam Part A 30:356-364. https://doi.org/10.1080/19440049.2012.742573

Lindorff-Larsen K, Piana S, Palmo K, Maragakis P, Klepeis JL, Dror RO, Shaw DE (2010) Improved side-chain torsion potentials for the Amber ff99SB protein force field. Proteins 78:1950-1958. https://doi.org/10.1002/prot.22711

Ma L, Maragos CM, Zhang Y (2018) Interaction of zearalenone with bovine serum albumin as determined by fluorescence quenching. Mycotoxin Res 34:39-48. https://doi.org/10.1007/s12550-017-0297-7

Maragos CM (2010) Zearalenone occurrence and human exposure. World Mycotoxin J 3:369-383. https://doi.org/10.3920/WMJ2010.1240.

Minervini F, Dell'Aquila ME (2008) Zearalenone and reproductive function in farm animals. Int J Mol Sci 9:2570-2584. https://doi.org/10.3390/ijms9122570.

Morris GM, Huey R, Lindstrom W, Sanner MF, Belew RK, Goodsell DS, Olson AJ (2009) AutoDock4 and AutoDockTools4: automated docking with selective receptor flexibility. J Comput Chem 30:2785-2791. https://doi.org/10.1002/jcc.21256

Perry JL, Il'ichev YV, Kempf VR, McClendon J, Park G, Manderville RA, Rüker F, Dockal M, Simon JD (2003) Binding of ochratoxin A derivatives to human serum albumin. J Phys Chem B 107:6644-6647. https://doi.org/10.1021/jp034284w

Poór M, Kunsági-Máté S, Bencsik T, Petrik J, Vladimir-Kneževic S, Kőszegi T (2012) Flavonoid aglycones can compete with ochratoxin A for human serum albumin: A new possible mode of action. Int J Biol Macromol 51:279-283.

https://doi.org/10.1016/j.ijbiomac.2012.05.019

Poór M, Li Y, Matisz G, Kiss L, Kunsági-Máté S, Kőszegi T (2014) Quantitation of species differences in albumin-ligand interactions for bovine, human and rat serum albumins using fluorescence spectroscopy: A test case with some Sudlow's site I ligands. J Lumin 145:767-773.
https://doi.org/10.1016/j.jlumin.2013.08.059

Poór M, Lemli B, Bálint M, Hetényi C, Sali N, Kőszegi T, Kunsági-Máté S (2015) Interaction of citrinin with human serum albumin. Toxins 7:5155-5166.
https://doi.org/10.3390/toxins7124871

Poór M, Bálint M, Hetényi C, Gődér B, Kunsági-Máté S, Kőszegi T, Lemli B (2017a) Investigation of non-covalent interactions of aflatoxins (B1, B2, G1, G2, and M1) with serum albumin. Toxins 9:339.
https://doi.org/10.3390/toxins9110339

Poór M, Kunsági-Máté S, Bálint M, Hetényi C, Gerner Z, Lemli B (2017b) Interaction of mycotoxin zearalenone with human serum albumin. J Photochem Photobiol B 170:16-24.
https://doi.org/10.1016/j.jphotobiol.2015.07.009

Poór M, Boda G, Kunsági-Máté S, Needs PW, Kroon PA, Lemli B (2018) Fluorescence spectroscopic evaluation of the interactions of quercetin, isorhamnetin, and quercetin-3′-sulfate with different albumins. J Lumin 194:156-163.
https://doi.org/10.1016/j.jlumin.2017.10.024

Ross PD, Subramanian S (1981) Thermodynamics of protein association reactions: forces contributing to stability. Biochemistry 20:3096-3102. https://doi.org/10.1021/bi00514a017

Schollenberger M, Müller HM, Rüfle M, Suchy S, Plank S, Drochner W (2006) Natural occurrence of 16 fusarium toxins in grains and feedstuffs of plant origin from Germany. Mycopathologia 161:43-52. https://doi.org/10.1007/s11046-005-0199-7.

Schrödinger LLC (2013) Schrödinger Release 2013-3: SiteMap, Version 2.9 Schrödinger, LLC, New York, USA.

Shier WT, Shier AC, Xie W, Mirocha, CJ (2001) Structure-activity relationships for human estrogenic activity in zearalenone mycotoxins. Toxicon 39:1435-1438. https://doi.org/10.1016/S0041-0101(00)00259-2.

Stewart JJ (1990) MOPAC: A semiempirical molecular orbital program. J Comput Aided Mol Des 4:1-105.

Sueck F, Poór M, Faisal Z, Gertzen CGW, Cramer B, Lemli B, Kunsági-Máté S, Gohlke H, Humpf HU (2018) Interaction of Ochratoxin A and Its Thermal Degradation Product 2'R-Ochratoxin A with Human Serum Albumin. Toxins 10:E256. https://doi.org/10.3390/toxins10070256

538 Yamasaki K, Chuang VT, Maruyama T, Otagiri M (2013) Albumin-drug interaction and its
539 clinical implication. Biochim Biophys Acta 1830:5435-5443.
540 https://doi.org/10.1016/j.bbagen.2013.05.005
541
542 Yazar S, Omurtag GZ (2008) Fumonisins, trichothecenes and zearalenone in cereals. Int J Mol
543 Sci 9:2062-2090.
544 https://doi.org/10.3390/ijms9112062
545
546 Yuqin L, Guirong Y, Zhen Y, Caihong L, Baoxiu J, Jiao C, Yurong G (2014) Investigation of
547 the interaction between patulin and human serum albumin by a spectroscopic method, atomic
548 force microscopy, and molecular modeling. Biomed Res Int 2014:734850.
549 https://doi.org/10.1155/2014/734850
550
551
552 Zsila F (2013) Subdomain IB is the third major drug binding region of human serum albumin:
553 Toward the three-sites model. Mol Pharm 10:1668-1682.
554 https://doi.org/10.1021/mp400027q

List of figures:

Fig. 1 Chemical structures of zearalenone, α-zearalenol, and β-zearalenol

Fig. 2 Stern-Volmer plots of mycotoxin complexes formed with HSA (a), BSA (b), PSA (c), and RSA (d) (λ_{ex} = 295 nm, λ_{em} = 340 nm; ZEN: zearalenone, α-ZEL: α-zearalenol, β-ZEL: β-zearalenol, HSA: human serum albumin, BSA: bovine serum albumin, PSA: porcine serum albumin, RSA: rat serum albumin)

Fig. 3 HPAC chromatograms of β-ZEL, α-ZEL, and ZEN eluted from the HSA-coated column (see details in *High performance affinity chromatography (HPAC)* section)

Fig. 4 The van't Hoff plots of zearalenone-albumin complexes (ZEN: zearalenone, HSA: human serum albumin, BSA: bovine serum albumin, PSA: porcine serum albumin, RSA: rat serum albumin)

Fig. 5 Binding constants of ZEN-HSA and ZEN-BSA complexes plotted against the ionic strength of the applied phosphate buffer at 298 K (ZEN: zearalenone, HSA: human serum albumin, BSA: bovine serum albumin)

Fig. 6 A: Zearalenone conformation and binding site on human albumin, as described in our previous study (Poór et al. 2017b). B: α-Zearalenol conformation and binding site on human albumin obtained in the first rank of blind docking calculation. C: β-Zearalenol conformation and binding site on human albumin obtained in the seventh rank of blind docking calculation

Fig. 7 First (Rank 1) and seventh (Rank 7) rank binding sites of β-zearalenol on human albumin based on blind docking

Fig. 8 Fluorescence emission intensity of warfarin (1 μmol/L; 0.308 mg/L) complexed with HSA (3.5 μmol/L; 0.233 g/L) in the presence of increasing zearalenone or zearalenol concentrations in PBS (pH 7.4; λ_{ex} = 317 nm, λ_{em} = 379 nm; ZEN: zearalenone, α-ZEL: α-zearalenol, β-ZEL: β-zearalenol)

580 **Tables**

581 **Table 1** Decimal logarithmic values of the Stern-Volmer quenching constants (K_{SV}; unit:

582 L/mol) and binding constants (K; unit: L/mol) of mycotoxin-albumin complexes

Mycotoxin-albumin complex*	**logK_{SV}** ± SD (unit of K_{SV}: L/mol)	**log$K$** ± SD (unit of K: L/mol)
ZEN-HSA	5.09 ± 0.01	5.09 ± 0.01
ZEN-BSA	4.81 ± 0.01	4.78 ± 0.01
ZEN-PSA	4.56 ± 0.02	4.57 ± 0.01
ZEN-RSA	5.50 ± 0.01	5.42 ± 0.00
α-ZEL-HSA	4.70 ± 0.02	4.72 ± 0.00
α-ZEL-BSA	4.54 ± 0.02	4.46 ± 0.02
α-ZEL-PSA	4.47 ± 0.07	4.49 ± 0.01
α-ZEL-RSA	5.32 ± 0.04	5.43 ± 0.00
β-ZEL-HSA	4.28 ± 0.04	4.33 ± 0.00
β-ZEL-BSA	4.27 ± 0.04	4.37 ± 0.01
β-ZEL-PSA	4.18 ± 0.07	4.05 ± 0.05
β-ZEL-RSA	5.29 ± 0.02	5.43 ± 0.00

583

584 *****(ZEN: zearalenone, α-ZEL: α-zearalenol, β-ZEL: β-zearalenol, HSA: human serum albumin,

585 BSA: bovine serum albumin, PSA: porcine serum albumin, RSA: rat serum albumin)

586 **Table 2** Thermodynamic parameters of zearalenone-albumin complexes (ZEN: zearalenone,
587 HSA: human serum albumin, BSA: bovine serum albumin, PSA: porcine serum albumin, RSA:
588 rat serum albumin). The parameters for the ZEN-HSA complex are from our earlier study (Poór
589 et al., 2017)

Thermodynamic parameters	**HSA**	**BSA**	**PSA**	**RSA**
ΔH (kJ mol^{-1})	–30.09	–3.13	–10.04	–34.20
ΔS (J K^{-1} mol^{-1})	–3.45	80.90	53.62	–10.65
$\mathbf{\Delta G_{298K}}$ (kJ mol^{-1})	–29.06	–27.25	–26.03	–31.03

590

591

592 **Table 3** The results of Uniprot alignment of BSA, PSA, and RSA with HSA (HSA: human
593 serum albumin, BSA: bovine serum albumin, PSA: porcine serum albumin, RSA: rat serum
594 albumin)

Comparison to HSA	**Identical Residues**	**Identity %**	**Residues**
HSA-BSA	465	76.34	106
HSA-PSA	462	75.86	99
HSA-RSA	446	73.23	128

595

Figures:

Fig. 1

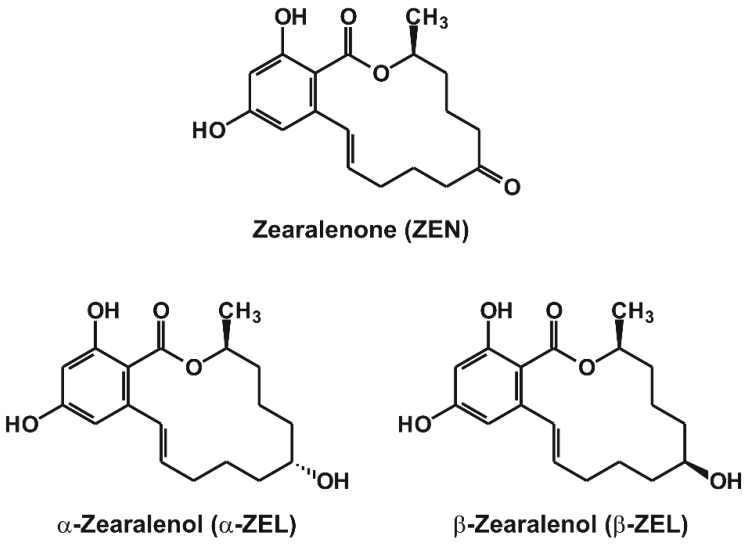

Fig. 2

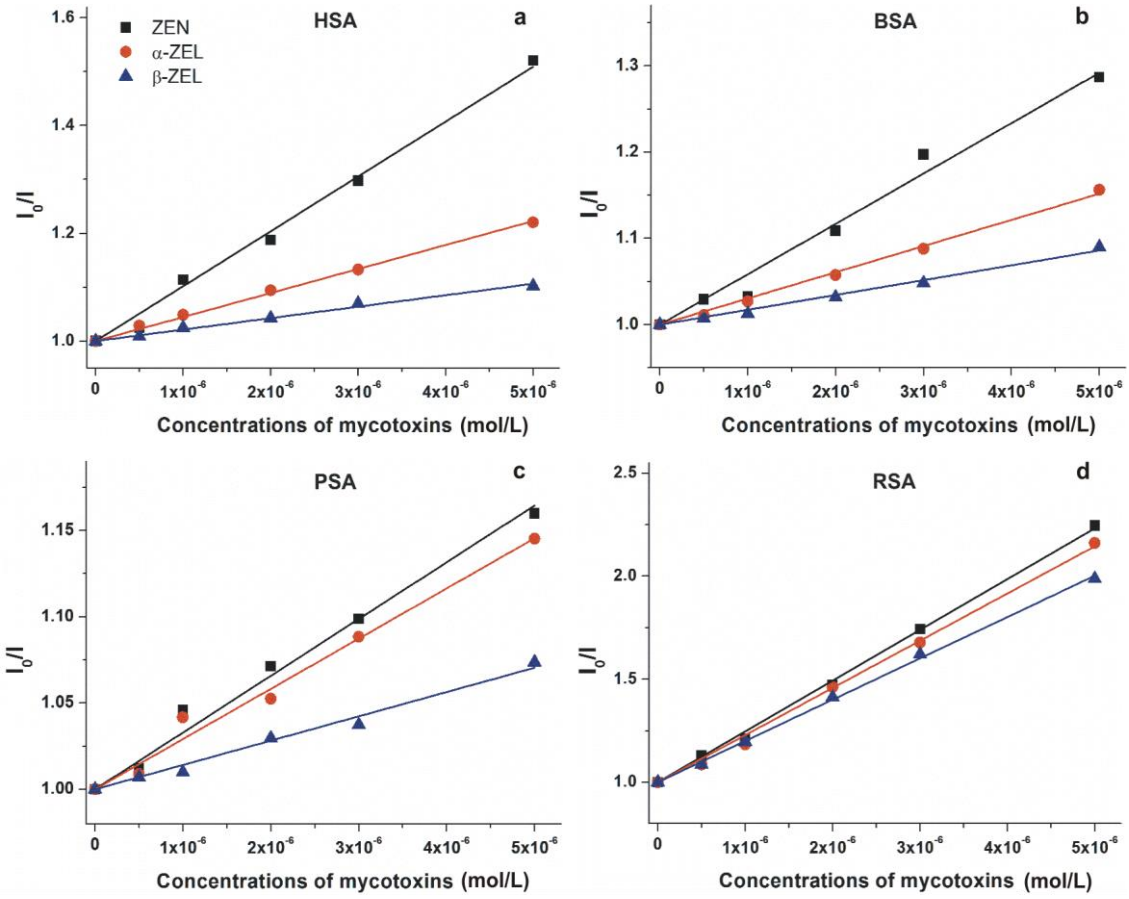

Fig. 3

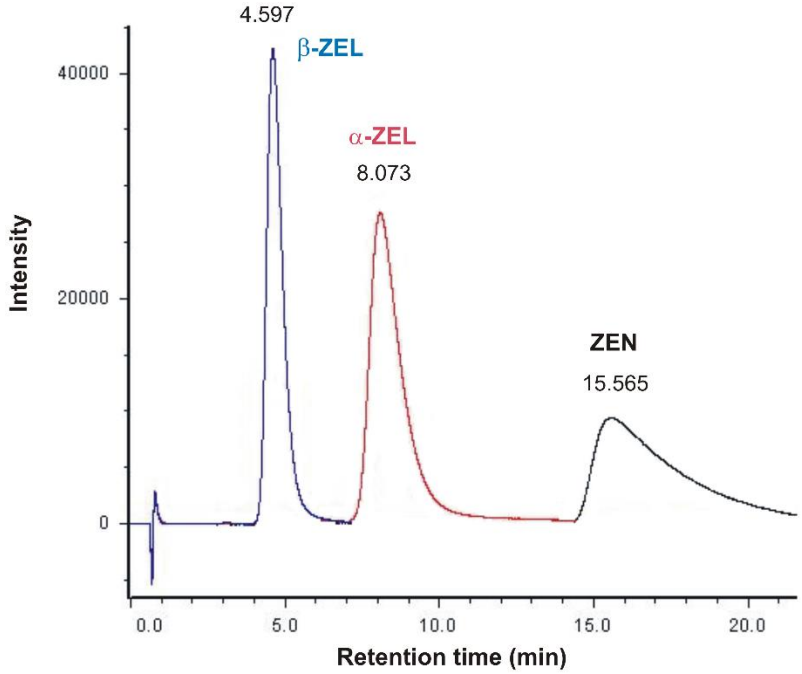
4.597
β-ZEL
α-ZEL
8.073
ZEN
15.565
Intensity
40000
20000
0
0.0
5.0
10.0
15.0
20.0
Retention time (min)

Fig. 4

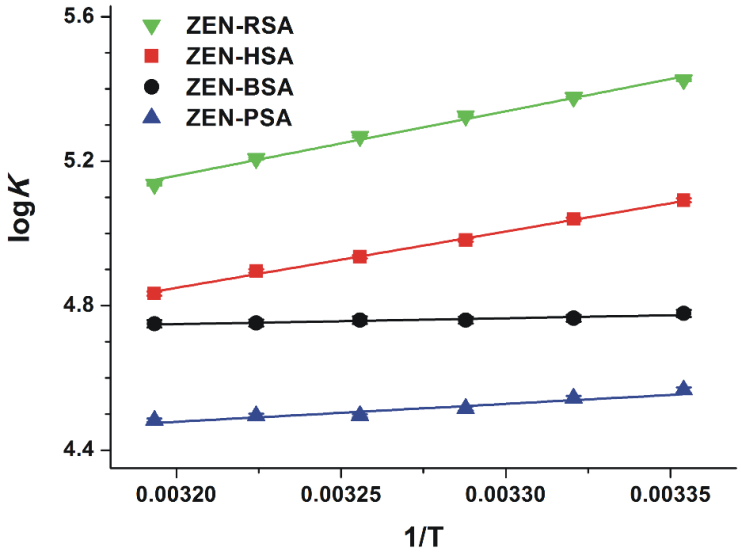
ZEN-RSA
ZEN-HSA
ZEN-BSA
ZEN-PSA
log K
5.6
5.2
4.8
4.4
0.00320
0.00325
0.00330
0.00335
1/T

614 ***Fig. 5***

615

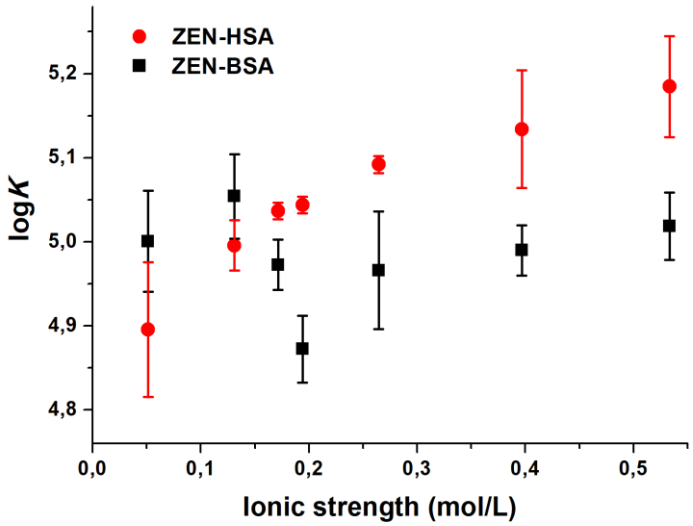

616

617

618

619 ***Fig. 6***

620

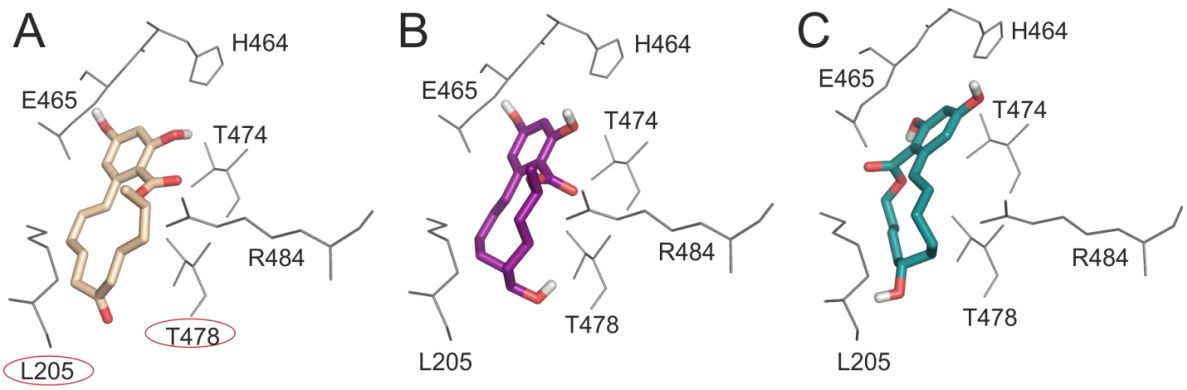

621

622

623

Fig. 7

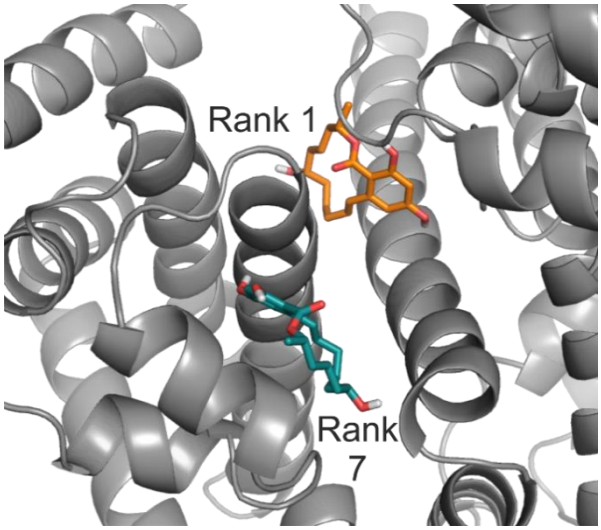
Rank 1
Rank 7

Fig. 8

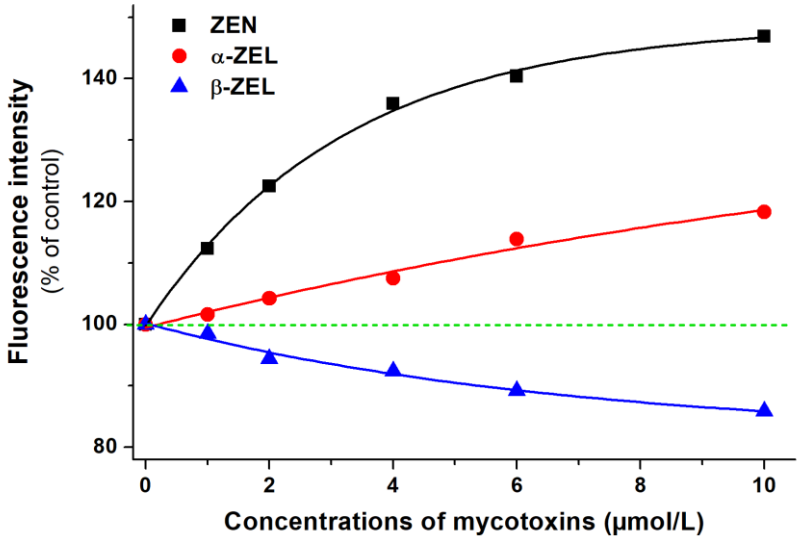
ZEN
α-ZEL
β-ZEL
Fluorescence intensity
(% of control)
140
120
100
80
0
2
4
6
8
10
Concentrations of mycotoxins (μmol/L)